

Damage Model Based Reinforced-Concrete Element

Chee Kiong Soh¹; Yu Liu²; Yue Xing Dong³; and Xin Zheng Lu⁴

Abstract: In this paper, the damage in concrete around a reinforcement bar is examined, and three types of damage in concrete and at the concrete-rebar interface are defined. Based on these definitions, a three-dimensional damaged reinforced-concrete (DRC) element is proposed. The element consists of a 10-node concrete element, a two-node rebar element, and a four-node concrete-rebar interface element. Experiments were carried out to obtain the parameters for the bond damage evolution equation. The proposed DRC element is implemented as a user-defined element of MSC MARC2000, a commercial finite-element analysis software package. Two numerical examples were examined, and the results show that the DRC element can simulate the bond deterioration in reinforced-concrete structural members with sufficient rationality, accuracy, and efficiency.

DOI: 10.1061/(ASCE)0899-1561(2003)15:4(371)

CE Database subject headings: Damage; Models; Concrete, reinforced.

Introduction

In the design and analysis of reinforced-concrete (RC) structures, the bond between the reinforcement bar (rebar) and concrete is one of the important factors that must be properly accounted for. The shear bond, in particular, is the main load-carrying mechanism between the concrete and its reinforcement in the longitudinal direction of the rebars. Although perfect bonding can be assumed when little or no stress transfer occurs between the concrete and rebar, slip at the concrete-rebar interface usually occurs when reinforced-concrete structures are loaded, especially in cases when high stress at the contact interface and at the end anchorage exists. It has been shown that it is essential to include bond-slip in the analysis of reinforced-concrete structures (Rots 1988). The bond stress is directly related to the slip of the interface. The behavior of the interface will deteriorate after the slip reaches a certain level, and as a result of damage development, nonlinear and softening behavior will appear in the bond stress-slip curves. These must be fully simulated in the reinforced-concrete structure analysis. While the various bond problems can be treated separately using contact elements (Ngo and Scordelis 1967; Schafer 1975; Herrmann 1978) or interface elements

(Stankowski et al. 1993a, b; Lourenço and Rots 1997; Soh et al. 1999), it is not easy to take into account the interaction between the cracking of concrete and the bond deterioration of the concrete-rebar interface. At the same time, these concrete-interface-rebar meshing techniques usually need many elements in the finite-element analysis (FEA) for accurate results to be obtained.

In this paper, a 12-node 3D damaged reinforced-concrete (DRC) element is developed based on the damage description of the concrete and the bond properties on the concrete-rebar interface. In this DRC element, the damage in the concrete and on the concrete-rebar interface is considered using three damage variables, so that the nonlinear and softening behavior of the concrete and the interface can be realistically modeled. Experiments were carried out to obtain the parameters for the bond damage evolution equation. The DRC element developed is implemented as a user-defined element in a commercial FEA package, MSC MARC2000 (User 1997). Two numerical examples are given to illustrate the effectiveness of the DRC element in analyzing reinforced-concrete specimens. The results show that the DRC element can simulate the bond deterioration in RC structural members with sufficient rationality and accuracy. However, the model is still too simple to deal with the complexity of real structures, and the limitations of the DRC element and required further work are discussed.

Reinforced-Concrete Element with Damage Description

In the 12-node 3D reinforced-concrete element developed, the concrete and the bond behavior of the concrete-rebar interface are described using damage mechanics. Thus, the element is called a damaged reinforced-concrete element or DRC element, in short. The DRC element consists of a 10-node brick element for the concrete, a two-node rod element for the rebar, and a four-node interface element for the interface between the concrete and rebar. One additional deformation mode of the concrete is introduced to account for the shear deformation of concrete due to the bond stress at the interface between the rebar and the concrete. The force-displacement relation of the additional deformation mode is

¹Professor, School of Civil and Environmental Engineering, Nanyang Technological Univ., Nanyang Ave., Singapore 639798. E-mail: csohck@ntu.edu.sg

²Research Scholar, School of Civil and Environmental Engineering, Nanyang Technological Univ., Nanyang Ave., Singapore 639798. E-mail: liuyu@pmail.ntu.edu.sg

³Research Fellow, School of Civil and Environmental Engineering, Nanyang Technological Univ., Nanyang Ave., Singapore 639798. E-mail: cyxdong@ntu.edu.sg or cyxdong@yahoo.com

⁴Exchange Student, Tsinghua Univ., Dept. of Civil Engineering, Beijing, People's Republic of China 100084. E-mail: luxz00@mails.tsinghua.edu.cn

Note. Associate Editor: Nemkumar Banthia. Discussion open until January 1, 2004. Separate discussions must be submitted for individual papers. To extend the closing date by one month, a written request must be filed with the ASCE Managing Editor. The manuscript for this paper was submitted for review and possible publication on July 18, 2001; approved on April 24, 2002. This paper is part of the *Journal of Materials in Civil Engineering*, Vol. 15, No. 4, August 1, 2003. ©ASCE, ISSN 0899-1561/2003/4-371-380/\$18.00.

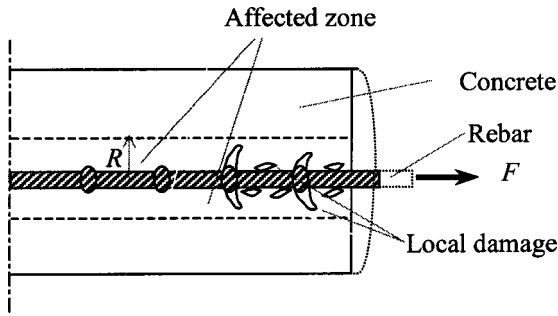


Fig. 1. Definition of affected zone

deduced using the principle of virtual work. Two scalar-damage variables, D_b and D_n , are introduced to describe the bond deterioration of the rebar-concrete interface and the cracking of the concrete. The derivation of the DRC element is explained in detail later.

Affected Zone and Local Damage

An affected zone is a volume of concrete around a deformed rebar in which local damage of concrete occurs as a result of the wedge action around the rebar, as shown in Fig. 1. As shown later, besides the deformation of the rebar, the deformation modes in the DRC element consist of the deformation modes of an eight-node isoparametric element, an additional shear deformation mode, and a slip mode at the concrete-rebar interface. Accordingly, three kinds of damage in the DRC element are identified, which are the local damage D_l in the affected zone of the concrete, the nonlocal damage D_n in the concrete, and the bond damage D_b at the rebar-concrete interface (Liu 2003). The local damage in the affected zone of the concrete is attributed to the additional deformation mode and the wedge action. The nonlocal damage in the concrete is attributed to the deformation modes of the eight-node isoparametric element. The bond damage indicates the deterioration of bond stiffness of the concrete-rebar interface because of the slip and wedge action around the rebar. For simplification, D_l , D_n , and D_b are all assumed to be scalars. Of the three kinds of damage, the local damage D_l is closely related to the bond damage D_b because they are due to wedge action around the rebar. So for simplification, the local damage D_l is assumed to be proportional to the bond damage D_b ; i.e.

$$D_l = \alpha D_b \quad (1)$$

where α = parameter that needs to be calibrated in the DRC element.

Additional Deformation Mode of Concrete in Damaged Reinforced-Concrete Element

To consider the shear deformation of the concrete around the rebar, an additional deformation mode in the affected zone is introduced, as shown in Fig. 2. The affected zone is assumed to be a concrete cylinder that is fixed at its rim and subjected to a force F_A along the x -axis on one end surface. The longitudinal axis of the cylinder is assumed to be the x -axis. Hence, in the r - θ - x coordinate system, the displacement field $u(x, r)$ can be assumed to be

$$u(x, r) = \delta_1 \frac{R}{R - R_s} \left(1 - \frac{x}{l} \right) \left(1 - \frac{r}{R} \right) \quad (2)$$

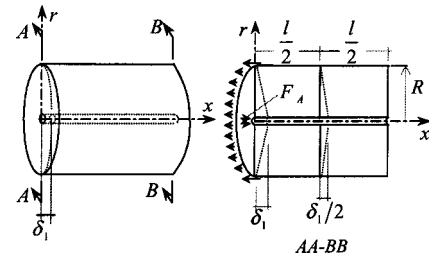


Fig. 2. Additional deformation mode of concrete

where R = radius of the affected zone; R_s = radius of the rebar; l = length of the concrete cylinder; and δ_1 = displacement of the interface relative to the rim at the loaded end of the DRC element.

According to the theory of elasticity, the idealized strain field can be derived as

$$\begin{aligned} \varepsilon_x &= \frac{\partial u}{\partial x} = -\frac{\delta_1}{l} \frac{1}{R - R_s} (R - r) \\ \varepsilon_{rx} = \varepsilon_{xr} &= \frac{1}{2} \frac{\partial u}{\partial r} = -\frac{1}{2} \frac{\delta_1}{R - R_s} \left(1 - \frac{x}{l} \right); \text{ others} = 0 \end{aligned} \quad (3)$$

and the stress fields are

$$\begin{aligned} \sigma_x &= E_c \frac{1 - \nu}{(1 + \nu)(1 - 2\nu)} \varepsilon_x; \quad \sigma_{rx} = \sigma_{rx} = E_c \frac{1}{(1 + \nu)} \varepsilon_{rx} \\ \sigma_r = \sigma_\theta &= E_c \frac{\nu}{(1 + \nu)(1 - 2\nu)} \varepsilon_x; \quad \text{others} = 0 \end{aligned} \quad (4)$$

where E_c and ν = elastic modulus and Poisson's ratio of the virgin concrete, respectively.

According to the principle of virtual work, the following equation can be written:

$$\int_{\Omega} (\sigma_x \tilde{\varepsilon}_x + \sigma_{rx} \tilde{\varepsilon}_{rx} + \sigma_{xr} \tilde{\varepsilon}_{xr}) d\Omega = F_A \tilde{\delta}_1 \quad (5)$$

where $\tilde{\varepsilon}_x = -(\tilde{\delta}_1/l)(R - r)/(R - R_s)$; $\tilde{\varepsilon}_{rx} = \tilde{\varepsilon}_{xr} = -0.5\tilde{\delta}_1(1 - x/l)/(R - R_s)$; and $\tilde{\delta}_1$ = virtual displacement. From Eqs. (4) and (5), the force-displacement relations can be derived as

$$\begin{aligned} F_A &= \frac{\pi E_c}{6(1 + \nu)} \frac{1}{(R - R_s)^2} \left[\frac{1 - \nu}{1 - 2\nu} (R^4 - 6R^2 R_s^2 + 8R R_s^3 - e R_s^4) \frac{1}{l} \right. \\ &\quad \left. + (R^2 - R_s^2) l \right] \delta_1 = K_r \cdot \delta_1 \end{aligned} \quad (6)$$

Bond Damage on Concrete-Rebar Interface

An accepted practice in dealing with the bond problem is to assume that the shear stress is a function of the slip of the interface with a damage factor included in the expression to take into account the degradation of the bond (Soh et al. 1999). The relationship between the bond stress and slip of the concrete-rebar interface is assumed to be

$$\tau(x) = E_b (1 - D_b) \Delta(x) \quad (7)$$

where E_b = virgin bond stiffness; D_b = mean bond damage in the DRC element; and $\Delta(x)$ = slip along the rebar. In Eq. (7), it is assumed that the bond behavior would deteriorate only when slip develops, but according to experimental observation (Maekawa

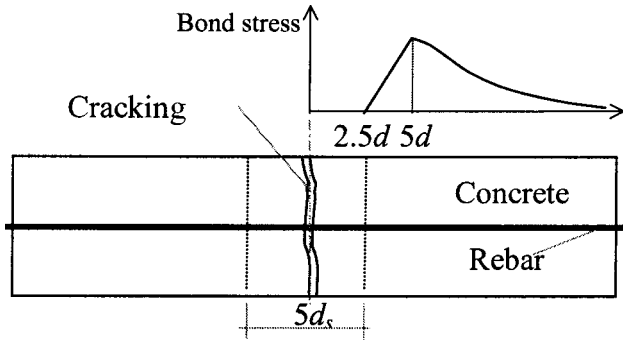


Fig. 3. Bond deterioration near cracking plane (Maekawa and Qureshi 1997)

and Qureshi 1997), the cracking of concrete will also affect the bond behavior. To account for this effect, a bond stress-slip relation is thus assumed

$$\tau(x) = E_b(1 - D_b)(1 - \beta D_n)\Delta(x) \quad (8)$$

where parameter β is related to the length of the DRC element, l . Maekawa and Qureshi (1997) assumed that the bond stress decreases to zero within a distance of $2.5d_s$ from the cracking plane (d_s is the diameter of the rebar), as shown in Fig. 3; so when $l < 5d_s$, we assume that $\beta = 1$.

A linear slip field is assumed for the DRC element, which can be written as

$$\Delta(x) = \Delta_1(1 - x/l) + \Delta_2(x/l) \quad (9)$$

where Δ_1 and Δ_2 = slip at the two ends of the DRC element, as shown in Fig. 4(a). The bond forces at the ends of the DRC element can then be calculated by

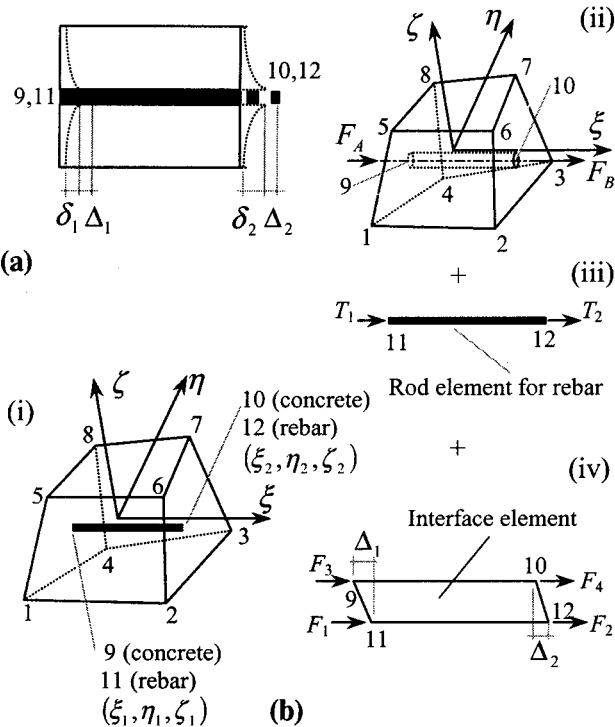


Fig. 4. Construction of 12-node DRC element: (a) deformation of DRC element; (b) assembly of DRC element ($i = ii + iii + iv$)

$$\begin{aligned} F_{b1} &= \int_0^l E_b(1 - D_b)(1 - \beta D_n)\Delta_1 \left(1 - \frac{x}{l}\right) \pi d_s dx \\ &= \frac{l}{2} \pi d_s E_b(1 - D_b)(1 - \beta D_n)\Delta_1; \\ F_{b2} &= \int_0^l E_b(1 - D_b)(1 - \beta D_n)\Delta_2 \left(\frac{x}{l}\right) \pi d_s dx \\ &= \frac{l}{2} \pi d_s E_b(1 - D_b)(1 - \beta D_n)\Delta_2 \end{aligned} \quad (10)$$

Eq. (10) can be used to determine experimentally the evolution equation of the bond damage D_b . For example, when a rebar is pulled out from the concrete, the pullout force, F_p , can be derived from Eq. (10) to be

$$F_p = F_{b1} + F_{b2} = \frac{l}{2} \pi d_s E_b(1 - D_b)(1 - \beta D_n)(\Delta_1 + \Delta_2) \quad (11)$$

Thus, the relationship between the bond damage D_b and the slip can be determined if the pullout force F_p and the slip on the two surfaces, Δ_1 and Δ_2 , can be measured and if it is ensured that $D_n = 0$ in the experiment.

Nonlocal Damage in Concrete

The nonlocal damage in concrete, D_n , in this paper refers to the degradation and cracking of concrete not directly induced by the bond damage or wedge action on the concrete-rebar interface. It occurs not only in the reinforced-concrete element, but also in the pure concrete element, and in the DRC element it is due to the deformation modes of the common eight-node isoparametric element of the concrete.

For simplification, a scalar damage model for concrete is adopted, with the stress-strain relationship defined as

$$\sigma' = (1 - D_n) \cdot \mathbf{D}^e \cdot \epsilon' \quad (12)$$

where $\sigma' = \{\sigma_{11} \sigma_{22} \sigma_{33} \sigma_{12} \sigma_{23} \sigma_{13}\}^T$ and $\epsilon' = \{\epsilon_{11} \epsilon_{22} \epsilon_{33} 2\epsilon_{12} 2\epsilon_{23} 2\epsilon_{13}\}^T$ = stress and strain vector, respectively; \mathbf{D}^e = elastic matrix; and D_n = damage scalar defined as

$$D_n = \begin{cases} 0, & \sigma_1^e \leq f_t \\ (1 - E_2/E_c)(1 - f_t/\sigma_1^e), & f_t < \sigma_1^e < (1 - E_c/E_2)f_t \\ 1, & \sigma_1^e \geq (1 - E_c/E_2)f_t \end{cases} \quad (13)$$

where $E_2 (< 0)$ = softening module; f_t = tensile strength of the concrete; and σ_1^e = maximum principal stress when the concrete is assumed to be an elastic material; that is

$$\sigma_1^e = \frac{1}{E_c(1 + \nu)(1 - 2\nu)} [(1 - \nu)\epsilon_1 + \nu(\epsilon_2 + \epsilon_3)] \quad (14)$$

where $\epsilon_1, \epsilon_2, \epsilon_3$ = principal strains. For the one-dimensional cases, this model gives a stress-strain curve as shown in Fig. 5, which is the same as those given by the crack band (or smear crack) model with a linear softening phase (Bazant and Oh 1983). But this model, described using damage mechanics, makes it easier to consider the interaction between the concrete cracking and the bond deterioration, as shown in Eq. (8).

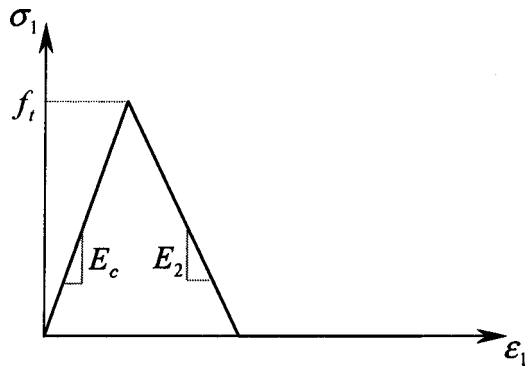


Fig. 5. Stress-strain curve of concrete (one dimension)

Secant Stiffness Matrix of Damaged Reinforced-Concrete Element

As shown in Fig. 4(b), the DRC element is composed of a 10-node concrete element, a two-node rebar element, and a four-node lumped interface element. Consider an eight-node isoparametric element with stiffness matrix \mathbf{K}^8 ; its force-displacement relationship is

$$\mathbf{F}^8 = \mathbf{K}^8 \cdot \mathbf{u}^8 \quad (15)$$

where \mathbf{F}^8 and \mathbf{u}^8 = nodal force and nodal displacement vector, respectively. Assuming that axis ξ is parallel to axis x , which is the direction of the rebar, the new force-displacement relationship considering the additional deformation mode of concrete can be expanded to

$$\mathbf{F}^c = \begin{Bmatrix} F_1^8 \\ \vdots \\ F_{24}^8 \\ F_A \\ F_B \end{Bmatrix} = (1 - D_n)(1 - \alpha D_b) \times \begin{bmatrix} K_{1,1}^c & \cdots & K_{1,24}^c & K_{1,25}^c & K_{1,26}^c \\ \vdots & \ddots & \vdots & \vdots & \vdots \\ K_{24,1}^c & \cdots & K_{24,24}^c & K_{24,25}^c & K_{24,26}^c \\ K_{25,1}^c & \cdots & K_{25,24}^c & K_r & K_{25,26}^c \\ K_{26,1}^c & \cdots & K_{26,24}^c & K_{26,25}^c & K_r \end{bmatrix} \begin{Bmatrix} u_1^8 \\ \vdots \\ u_{24}^8 \\ \delta_1 \\ \delta_2 \end{Bmatrix} = (1 - D_n)(1 - \alpha D_b) \mathbf{K}^c \cdot \mathbf{u}^c \quad (16)$$

in which

$$\begin{Bmatrix} F_1^8 \\ \vdots \\ F_{24}^8 \\ F_A + F_3 \\ F_B + F_4 \\ F_1 + T_1 \\ F_2 + T_2 \end{Bmatrix} = \begin{bmatrix} K_{1,1} & \cdots & K_{1,24} & K_{1,25} & K_{1,26} & 0 & 0 \\ \vdots & \ddots & \vdots & \vdots & \vdots & \vdots & \vdots \\ K_{24,1} & \cdots & K_{24,24} & K_{24,25} & K_{24,26} & 0 & 0 \\ K_{25,1} & \cdots & K_{25,24} & K_{25,25} + K_{sd} & 0 & -K_{sd} & 0 \\ K_{26,1} & \cdots & K_{26,24} & 0 & K_{26,26} + K_{sd} & 0 & -K_{sd} \\ 0 & \cdots & 0 & -K_{sd} & 0 & K_{sd} + K_{ss} & -K_{ss} \\ 0 & \cdots & 0 & 0 & -K_{sd} & -K_{ss} & K_{sd} + K_{ss} \end{bmatrix} \begin{Bmatrix} u_1^8 \\ \vdots \\ u_{24}^8 \\ \delta_1 \\ \delta_2 \\ \delta_1 + \Delta_1 \\ \delta_2 + \Delta_2 \end{Bmatrix} \quad (19)$$

$$K_{i,j}^c = \begin{cases} K_{i,j}^8 + \lambda_i \lambda_j K_r + \lambda_i' \lambda_j' K_r, & i, j \in S_x \\ K_{i,j}^8, & \text{others,} \end{cases}$$

$$K_{25,j}^c = K_{i,25}^c = \begin{cases} -\lambda_i K_r, & i \in S_x \\ 0, & \text{others} \end{cases}$$

$$K_{26,i}^c = K_{i,26}^c = \begin{cases} -\lambda_i' K_r, & i \in S_x \\ 0, & \text{others} \end{cases}$$

$$\lambda_i = N_{i+2/3}(\xi_1, \eta_1, \zeta_1)$$

$$\lambda_i' = N_{i+2/3}(\xi_2, \eta_2, \zeta_2)$$

where $N_i(\xi, \eta, \zeta)_{i=1, \dots, 8}$ = shape function of the eight-node isoparametric element; and set $S_x = \{1, 4, 7, 10, 13, 16, 19, 22\}$ consists of the indices denoting the degree of freedom in the x -direction. Because the local damage $D_l = \alpha D_b$ only occurs in the affected zone, as in Eq. (10), the size of the DRC element has been limited to be just the size of the affected zone.

The force-displacement relationship of the two-node rebar element can be written as

$$\mathbf{F}^s = \begin{Bmatrix} T_1 \\ T_2 \end{Bmatrix} = \frac{E_s A_s}{l} \begin{bmatrix} 1 & -1 \\ -1 & 1 \end{bmatrix} \begin{Bmatrix} \Delta_1 + \delta_1 \\ \Delta_2 + \delta_2 \end{Bmatrix} = \mathbf{K}^s \cdot \mathbf{u}^s \quad (17)$$

where E_s and A_s = elastic modulus and cross-sectional area of the rebar, respectively.

In fact, Eq. (10) also defines the force-displacement relationship of the four-node lumped interface element (Rots 1988), which can be expressed as

$$\mathbf{F}^b = \begin{Bmatrix} F_1 \\ F_3 \\ F_2 \\ F_4 \end{Bmatrix} = (1 - D_b)(1 - \beta D_n) \frac{l}{2} \pi d_s E_b \times \begin{bmatrix} 1 & -1 & 0 & 0 \\ -1 & 1 & 0 & 0 \\ 0 & 0 & 1 & -1 \\ 0 & 0 & -1 & 1 \end{bmatrix} \begin{Bmatrix} \delta_1 + \Delta_1 \\ \delta_1 \\ \delta_2 + \Delta_2 \\ \delta_2 \end{Bmatrix} = (1 - D_b)(1 - \beta D_n) \mathbf{K}^b \cdot \mathbf{u}^b \quad (18)$$

Using Eqs. (16)–(18), the secant stiffness matrix of the DRC element can readily be assembled as follows:

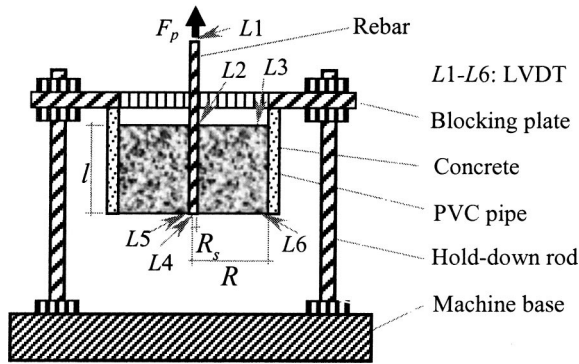


Fig. 6. Experimental setup

in which

$$K_{i,j} = (1 - D_n)(1 - \alpha D_b) K_{i,j}^c; \quad i, j = 1, \dots, 26$$

$$K_{sd} = 0.5\pi l d_s E_b (1 - D_b)(1 - \beta D_n); \quad K_{ss} = E_s A_s / l$$

Experimental Calibration

As mentioned earlier, one important issue in developing the DRC element is to model the bond behavior of the concrete-rebar interface, as expressed in Eq. (8). In the equation, the damage scalar D_b is introduced to account for the deterioration of the bond characteristics. If the evolution equation of D_b is known, the behavior of the interface can be correctly described with Eq. (8). Hence, the purpose of the experimental test is to determine the evolution equation of D_b . According to Eq. (11), the evolution equation can be obtained from the experimentally recorded $F_p \sim \Delta$ curve.

Experimental Setup

The specimen is cylindrical in shape, with a rebar ($d_s = 10$ mm) embedded along the central axis. In the derivation of Eq. (11), we have assumed that the damage state of the interface could be represented by a mean damage, D_b . So, the thickness of the specimen should be as thin as possible. Thus, the thickness of the specimen is designed to be 75 mm, as the maximum size of coarse aggregates is 20 mm. The loading device was designed as shown in Fig. 6. A hole, with the same size as the concrete specimen, is made in the center of the steel blocking plate, which is fixed to the base of the tension machine, Instron 4486, by four steel hold-down rods. Special glue was used to stick the specimen to a polyvinyl chloride (PVC) pipe, which was cut into eight pieces to eliminate the lateral confinement effect (Malvar 1992). So when the rebar is pulled upward, the PVC pipe will be held back by the blocking plate. The maximum tension stress in the specimen is much less than f_t , so according to Eq. (13), the nonlocal damage D_n is ensured to be zero. More details on the experimental study can be found in Lu (2000).

Experimental Results

A total of two groups of 13 specimens, with diameters of $d_s = 10$ cm (Group 10) and 15 cm (Group 15), respectively, were tested. Some typical failed specimens are shown in Fig. 7. Apparently, all of the specimens failed with major longitudinal radial

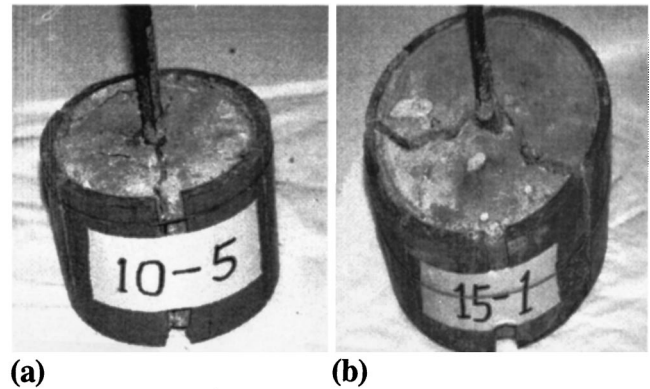


Fig. 7. Typical failure modes of tested specimens: (a) Specimen 10-5; (b) Specimen 15-1

cracks (splitting failure). The process of failure was observed as follows. First, when the load approached its peak value, the radial cracks started appearing on the top surface of the concrete around the steel bar. The cracks extended very fast, and soon they ran through the top surface and extended downward along the side of the specimen. The stiffness of the specimen decreased quickly when the cracks ran through the top surface. When the load reached the peak, the cracks extended so fast that the linear variable differential transducers could not properly record this process. The speed of the downward extension of the cracks varied from specimen to specimen. Generally, the larger the specimen, the quicker the cracks extended.

The experimental bond stress-slip curves for the Group 10 and Group 15 specimens are shown in Figs. 8(a and b), in which τ is the average bond stress, Δ_1 is the relative displacement of the steel bar and concrete on the top surface, and Δ_2 is that of the bottom surface. It is apparent that the bond stress-slip curves from the six Group 10 specimens are similar except for the one from Specimen 10-4, which suffered a sudden crash of the experimental setup for some unknown reason. The results from the seven Group 15 specimens are more scattered compared to those from the Group 10 specimens. As mentioned earlier, the cracks in the Group 15 specimens extended so fast that the bond stress decreased abruptly after the peak. The second peaks observed in some of the curves may be because the stiffness of the loading system was inadequate.

To fit the experimental results, the evolution equation of the bond damage is assumed to be

$$D_b = \begin{cases} 0, & \Delta \leq \gamma \\ \left(1 - \frac{\tau_r}{E_b \Delta}\right) \left(1 - \exp\left[-\frac{1}{a}(\Delta - \gamma)^m\right]\right), & \Delta > \gamma \end{cases} \quad (20)$$

where $\Delta = 0.5(\Delta_1 + \Delta_2)$; τ_r = residual bond strength; γ = damage threshold; and parameters a, m can be determined from

$$m = -\frac{\Delta_0 - \gamma}{(\Delta_0 - \tau_r / E_b) \ln \frac{\tau_0 - \tau_r}{E_b \Delta_0 - \tau_r}}$$

$$a = m \left(\Delta_0 - \frac{\tau_r}{E_b}\right) (\Delta_0 - \gamma)^{m-1} \quad (21)$$

where τ_0 and Δ_0 = bond strength and corresponding slip value, respectively. In fact, Eq. (20) is a translation on a Weibull cumulative distribution function (D_b'), as shown in Fig. 9. As shown in

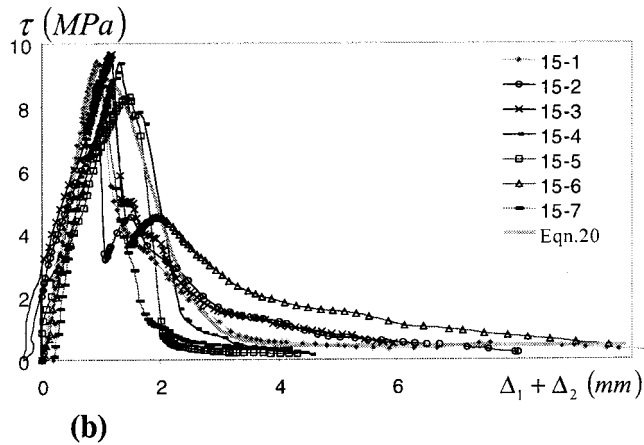
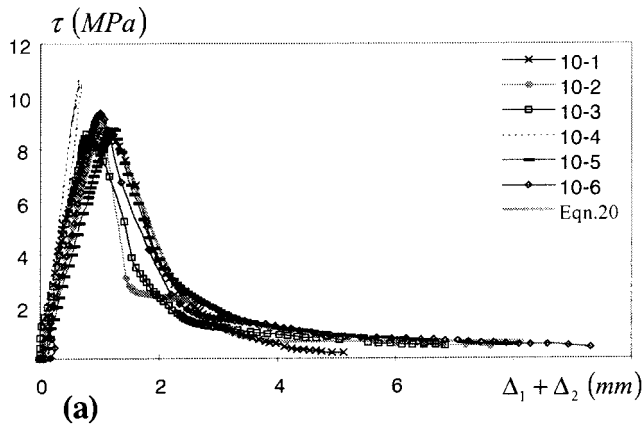


Fig. 8. Bond stress-slip curves of specimens: (a) bond stress-slip curves of Specimen Group 10; (b) bond stress-slip curves of Specimen Group 15

Figs. 8(a and b), the fitted bond stress-slip curves for Group 10 and Group 15 using Eq. (20) generally agree well with the experimental results.

Numerical Examples

In this section, the developed DRC element is used to model the specimens tested in the experiment. The computed mean bond stress-slip relations from two meshes are compared with the experimental results. The DRC element is next used to analyze the

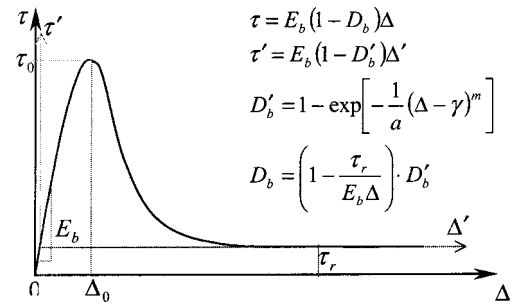


Fig. 9. Bond damage and bond stress-slip curve

specimen used in the uniaxial-tension test of Doerr (Keuser and Mehlhorn 1987), whereby the distribution of the tensile force along the rebar from two meshes is worked out and compared with the test results. The numerical results indicate that the DRC element is efficient and effective for practical applications.

Example 1: Specimen $d_s = 10$ cm

The specimen of Group 10 used in the experimental test was computed using the DRC element as its initial application. As shown in Fig. 10, the specimen was modeled using five elements in Model 1, consisting of one DRC element for the concrete-rebar and four ordinary eight-node brick elements for the rest of the concrete. In Model 2, two DRC elements and 16 eight-node brick elements were used. The eight-node brick elements are provided by MSC MARC2000 (Element Type 7), and the material type used is the “low tension material” whose stress-strain curve is similar to the one shown in Fig. 5 (“User” 1997). In MARC, the DRC element has been incorporated as a user-defined element, implemented using the user subroutine, uselem. The derivation of the tangent stiffness matrix of the DRC element required in uselem is given in Appendix I. The material parameters of the specimens were obtained from the experimental test, as shown in Table 1. The nodes at the rim of the top surface were fixed, and the tension force was applied on the rebar.

According to the experiments of Hayashi and Kokusho (1982), the radius of the affected zone, R , is about $2d_s$; the size of the DRC element is thus also $2d_s$, to make sure that the damage in the concrete is the same, as required in Eq. (16). In this study, it is assumed that when the rebar is pulled out, the concrete in the affected zone also failed. Hence, the parameter representing con-

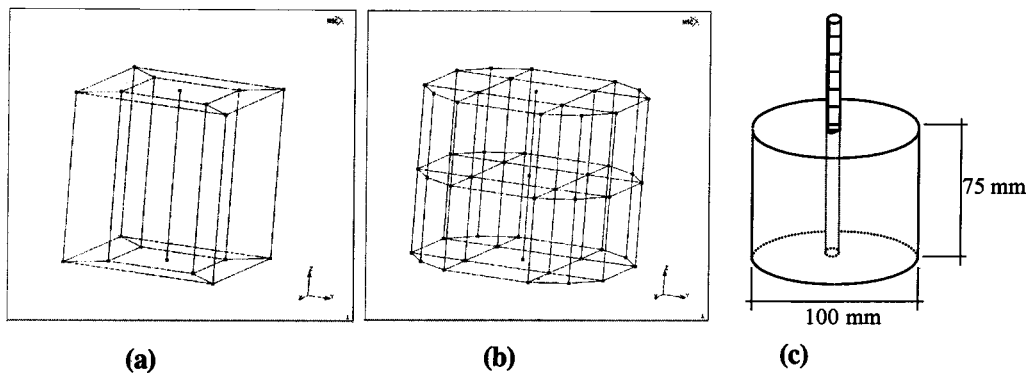


Fig. 10. Models of Group 10 specimens: (a) Model 1; (b) Model 2; (c) specimen

Table 1. Material Properties

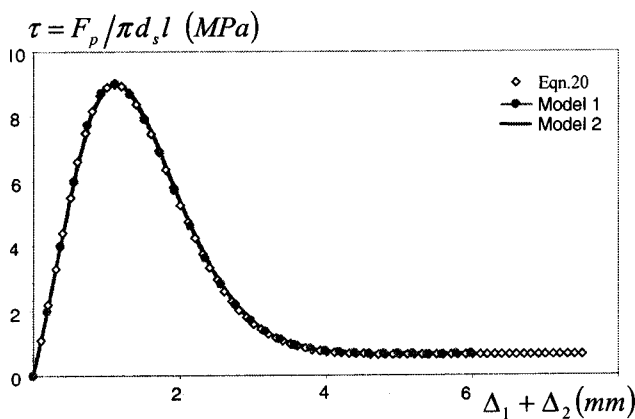
Example	Concrete	Rebar	Bond
1	$f_c = 30$ MPa $f_t = 2.9$ MPa $E_c = 22,000$ MPa $\nu_c = 0.2$	$f_y = 500$ MPa $E_s = 157,000$ MPa $d_s = 10$ mm	$\tau_0 = 9.0$ MPa $\Delta_0 = 0.55$ mm $E_b = 22$ N/mm ³ $\tau_r = 0.63$ MPa $\gamma = 0.2950$ mm
2	$f_c = 37.2$ MPa $f_t = 2.7$ MPa $E_c = 35,000$ MPa $E_2 = \begin{cases} -3.5 \times 10^5 & \text{MPa (Model 1)} \\ -1.7 \times 10^5 & \text{MPa (Model 2)} \end{cases}$ $\nu_c = 0.2$	$f_y = 420$ MPa $E_s = 205,000$ MPa $d_s = 16$ mm	$\tau_0 = 6.075$ MPa $\Delta_0 = 0.233$ mm $E_b = 35$ N/mm ³ $\tau_r = 0.425$ MPa $\gamma = 0.109$ mm

crete weakening induced by the bond damage, α , is set to be 1 when the size of the DRC element is the same as the size of the affected zone R .

As shown in Fig. 11, the mean bond stress-slip curves computed from the two models are then compared with the one fitted from the experimental data using Eq. (20) [which has been shown in Fig. 8(a)]. It is apparent that the developed DRC element can be used to accurately simulate the bond stress-slip relationship of the concrete and rebar interface.

Example 2: Doerr's Uniaxial-Tension Test

The DRC element is also used to simulate Doerr's uniaxial-tension test of a reinforced-concrete specimen (Keuser and Mehlhorn 1987). As shown in Fig. 12, half of the test specimen was discretized with DRC elements and eight-node brick elements. The material properties are also listed in Table 1, in which the maximum bond stress τ_0 was obtained from the Fédération Internationale de la Précontrainte model code for concrete structures ("Examples" 1990). Because the element length in Model 2 is about half of that in Model 1, the softening module in Model 2 is set to be about half of that in Model 1, so as to ensure a constant fracture energy of concrete (Bazant and Oh 1983). In this example, the result is not sensitive to the softening module of the concrete—perhaps because the process of concrete cracking was completed within one increment. The other parameters, which were determined from the experimental results in Example 1, are discussed in Appendix II.

**Fig. 11.** Computed and tested bond stress-slip curves

The applied tension force versus the displacement for both of the models was worked out and plotted in Fig. 13. The numerical results of the tensile force distribution along the rebar were compared with the test data in Fig. 14 for three load levels of tension force, $T = 20, 40,$ and 70 kN. Apparently, Model 2 with a fine mesh produced better agreement with the experimental results. It is noted that the computed profiles of the tension force when $T = 40$ and 70 kN, especially from Model 1, shifted slightly to the right as compared to the experimental results. This is because in the numerical computation, cracking of concrete can only occur in the first element from the symmetric plane, which induced the failure of the entire element; but in the actual experimental test, cracking just occurred on the symmetric plane. This difference is illustrated in Fig. 15.

In the computation using the DRC element, the test specimen has been modeled as a three-dimensional problem in which 20 and 50 linear elements are used in Model 1 and Model 2, respectively. Generally, the numerical results agree well with the test data. Compared to the traditional concrete-interface-rebar modeling, the DRC element appears to be more suitable for the 3D analysis of RC members. For example, in Keuser and Mehlhorn's (1987) computation on the aforementioned specimen, 23 eight-node axisymmetric quadratic isoparametric elements (concrete and rebar) plus five three-node quadratic contact elements (interface) were used, even though the axisymmetry of the specimen was considered to simplify it into a 2D problem. If the specimen cannot be simplified into a 2D problem, and must be analyzed as a 3D problem, a significantly large number of elements will be required to achieve the same accuracy.

Conclusions

Based on the identification of the three types of damage in the reinforced concrete and on the concrete-rebar interface, a damaged reinforced-concrete element was derived. In the DRC element, the material properties of the concrete and concrete-rebar interface were described using damage mechanics. This makes it easy to consider the interaction between the failure of the concrete and the bond deterioration of the interface, which has been difficult when using the traditional standard 3D modeling techniques (concrete-interface-rebar). An experimental test was carried out and an empirical bond damage evolution equation was derived from the test curves, which made it realistic to numerically compute the behavior of the reinforced concrete. Two numerical examples were presented using the developed DRC ele-

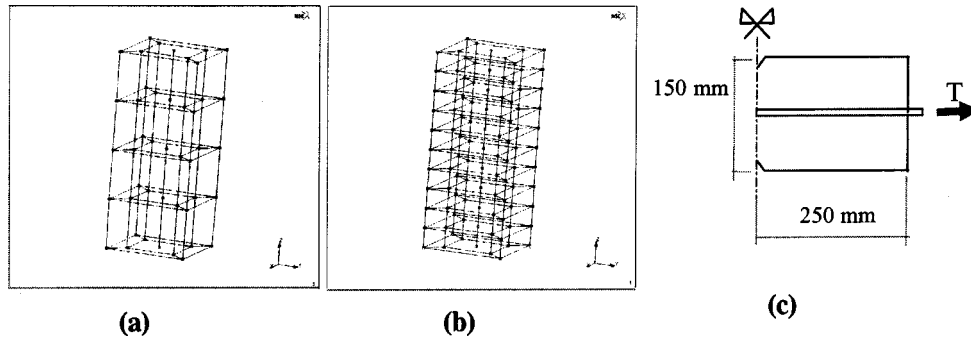


Fig. 12. Models of tested specimens: (a) Model 1; (b) Model 2; (c) specimen

ment, and their results suggested that the DRC element was able to accurately simulate certain behavior of the reinforced concrete.

However, the model is still too simple to deal with the complexity of real structures. In the developed DRC element, the size was limited to about $2d_s$. In addition, only one rebar was considered, and its direction was along an axis of the coordinate system. Unfortunately, these limitations on the size of the element and the number, as well as direction, of the rebars hindered the modeling. It should also be highlighted that the developed DRC element was useful only when a simple bond model was adopted; i.e., where the bond stress is only a function of its slip. For the more sophisticated and realistic bond models, where the bond stress also depends on its confinement, and the slip will lead to dilation of the concrete (Lundgren and Gylltoft 2000), the DRC element will need some generalizations. This will also be part of our future research work.

Appendix I: Tangent Stiffness Matrix of Damaged Reinforced-Concrete Element

Differentiating both sides of Eq. (16), we obtained

$$d\mathbf{F}^c = (1 - D_n)(1 - \alpha D_b) \mathbf{K}^c \cdot d\mathbf{u}^c - (1 - \alpha D_b) \mathbf{K}^c \cdot \mathbf{u}^c \cdot dD_n - \alpha(1 - D_n) \cdot \mathbf{K}^c \cdot \mathbf{u}^c \cdot dD_b \quad (22)$$

Differentiating both sides of Eq. (18), we obtained

$$d\mathbf{F}^b = (1 - D_b)(1 - \beta D_n) \mathbf{K}^b \cdot d\mathbf{u}^b - \beta(1 - D_b) \mathbf{K}^b \cdot \mathbf{u}^b \cdot dD_n - (1 - \beta D_n) \mathbf{K}^b \cdot \mathbf{u}^b \cdot dD_b \quad (23)$$

and from Eq. (13) we have

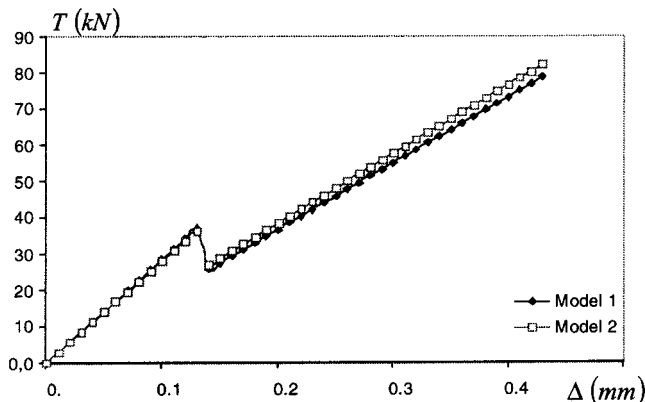


Fig. 13. Tension force versus displacement curves

$$dD_n = \begin{cases} 0, & \sigma_1^e \leq f \\ (1 - E_2/E_c) \frac{f_t}{(\sigma_1^e)^2} \frac{\partial \sigma_1^e}{\partial u^8} \cdot du^8, & f_t < \sigma_1^e < (1 - E_c/E_2)f_t \\ 0, & \sigma_1^e \geq (1 - E_c/E_2)f_t \end{cases} \quad (24)$$

where

$$\frac{\partial \sigma_1^e}{\partial u^8} = \frac{1}{E_c(1 - \nu)(1 - 2\nu)} [\nu, 1 - \nu, 1 - \nu] \cdot \frac{\partial \boldsymbol{\epsilon}^p}{\partial \boldsymbol{\epsilon}'} \cdot \mathbf{B}^8 \quad (25)$$

where matrix \mathbf{B}^8 = geometric matrix of the eight-node isoparametric element; and $\boldsymbol{\epsilon}^p = \{\epsilon_1 \ \epsilon_2 \ \epsilon_3\}^T$ = vector of principal strain, which can be computed by

$$\epsilon_i = \frac{1}{3} (\epsilon_{11} + \epsilon_{22} + \epsilon_{33}) + \frac{2}{\sqrt{3}} \cos \theta_i, \quad i = 1, 2, 3 \quad (26)$$

where $\theta_1 = \cos^{-1}(1.5\sqrt{3}J_3/J_2^{1.5})/3$; $\theta_2 = \theta_1 + 2\pi/3$; $\theta_3 = \theta_1 - 2\pi/3$; and J_2 and J_3 = second and third invariance of the deviatoric tensor of strain, \mathbf{e} , respectively. The derivatives of the principal strain with respect to the components of the strain tensor are

$$\frac{\partial \epsilon_k}{\partial \epsilon_{ij}} = \frac{1}{3} \delta_{ij} + \frac{1}{\sqrt{3}J_2} \cos(\theta_k) e_{ij} - \sqrt{\frac{4J_2}{4J_2^3 - 27J_3^2}} \times \sin(\theta_k) \left(\frac{3J_3}{2J_2} e_{ij} - e_{ip} e_{pj} + \frac{2}{3} J_2 \delta_{ij} \right) \quad (27)$$

with the summation convention on subscript p . From Eq. (21), we obtained

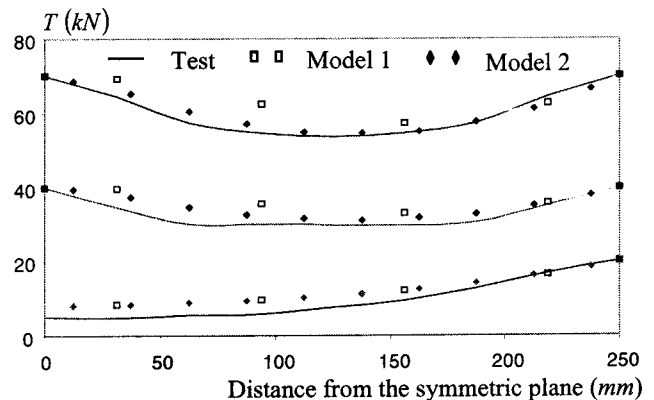


Fig. 14. Profile of tension force on rebar

$$dD_b = \begin{cases} 0, & x \leq \gamma \\ \left\{ \left[\left(1 - \frac{\tau_r}{E_b x} \right) \frac{m}{a} (x - \gamma)^{m-1} - \frac{\tau_r}{E_b x^2} \right] \exp \left[-\frac{1}{a} (x - \gamma)^m \right] + \frac{\tau_r}{E_b x^2} \right\} dx, & x > \gamma \end{cases} \quad (28)$$

where $dx = [-0.5 \ -0.5 \ 0.5 \ 0.5] \cdot d\mathbf{u}_b$.

In this paper, yielding of the rebar is not taken into account. Hence, from Eq. (17), we obtained

$$d\mathbf{F}^s = \mathbf{K}^s \cdot d\mathbf{u}^s \quad (29)$$

From Eqs. (22)–(29), the tangent stiffness matrix of the DRC element can thus be assembled.

Actually, we can describe the yielding of the rebar by simply introducing another damage scalar D_s ; i.e.

$$\mathbf{F}_s = (1 - D_s) \cdot \mathbf{K}^s \cdot d\mathbf{u}^s \quad (30)$$

$$D_s = \begin{cases} 0 & \text{when } |\Delta_2 + \delta_2 - \Delta_1 - \delta_1| \leq d_y \\ 1 - d_y / |\Delta_2 + \delta_2 - \Delta_1 - \delta_1| & \text{when } |\Delta_2 + \delta_2 - \Delta_1 - \delta_1| > d_y; \quad d_y = \frac{f_y}{E_s} l \end{cases} \quad (31)$$

where d_y = deformation of the rebar under yielding load; and f_y = yielding strength of the rebar. Hence, the tangent stiffness matrix of the DRC element, considering yielding of the rebar, can be obtained using the foregoing similar steps.

Appendix II: Discussion on Initial Bond Modulus E_b

Apparently, the initial bond modulus of the concrete-rebar interface is influenced by the properties of the concrete and the rebar—for instance, the concrete modulus and the shape of the rib of the ribbed bar. In Example 1, it has been found that the initial bond modulus obtained experimentally ($E_b = 2.2 \times 10^4$ MPa/m) is nearly the same as the tested initial modulus of the concrete ($E_c = 2.2 \times 10^4$ MPa). Hence, in Example 2, E_b is also tentatively set to be the same as E_c . To make sure that the bond stress-slip curves used in Example 1 and Example 2 are similar, it is assumed that

$$\frac{\tau_0^1}{E_b^1 \Delta_0^1} = \frac{\tau_0^2}{E_b^2 \Delta_0^2}; \quad \frac{\gamma^1}{\Delta_0^1} = \frac{\gamma^2}{\Delta_0^2}; \quad \frac{\tau_r^1}{\tau_0^1} = \frac{\tau_r^2}{\tau_0^2} \quad (32)$$

where superscripts 1 and 2 represent Example 1 and Example 2, respectively. The value $\tau_0/E_b \Delta_0$ reflects the damage state at the peak of the bond stress-slip curve, and the values γ/Δ_0 and τ_r/τ_0 decide the softening phase. In Example 2, the bond strength τ_0 was obtained from the code, and E_b is assumed to be the same value as E_c . So, x_0 , γ , and τ_r are all determined according to Eq. (32).

It should be mentioned that although the results obtained using the parameters determined previously are acceptable, this may be a coincidence. An experimentally obtained bond stress-slip curve is more reliable and preferred. Nevertheless, the relationships between E_b and E_c as well as other material properties still deserve more research work.

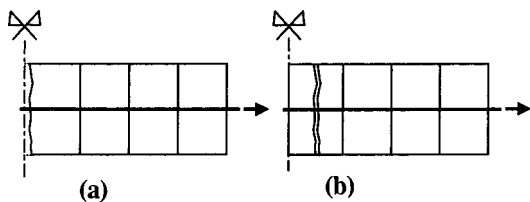


Fig. 15. Concrete cracking: (a) tested; (b) computed

Notation

The following symbols are used in this paper:

- A_s = cross-sectional area of rebar;
- a, m, γ = bond parameters;
- \mathbf{D}^e = elastic matrix of concrete;
- D_b = bond damage at rebar-concrete interface;
- D_l, D_n = local and nonlocal damage of concrete;
- D_s = damage of rebar;
- d_y = deformation of rebar under yielding load;
- E_b, E_c, E_s = stiffness of concrete, concrete-rebar interface, and rebar;
- E_2 = softening module of concrete;
- \mathbf{e} = deviatoric tensor of strain;
- F_b, F_p = bond forces and pullout force;
- f_t = tension strength of concrete;
- f_y = yielding strength of rebar;
- J_2, J_3 = second and third invariance of deviatoric tensor of strain;
- $\mathbf{K}^b, \mathbf{K}^c, \mathbf{K}^s$ = stiffness matrix of interface element, concrete element, and rebar element;
- \mathbf{K}^8 = stiffness matrix of eight-node brick element;
- l = length of damaged reinforced-concrete element;
- $N_{i \ i=1, \dots, 8}$ = shape function of eight-node brick element;
- R, R_s = radii of affected zone and rebar;
- T = tension force on rebar;
- u = displacement;
- α = parameter representing concrete weakening induced by bond damage;
- β = parameter representing bond deterioration due to concrete cracking;
- Δ = slip along rebar;
- Δ_0 = slip corresponding to bond strength;
- δ = displacement of interface as relative to rim of concrete cylinder;
- $\boldsymbol{\varepsilon}, \boldsymbol{\varepsilon}'$ = strain tensor and vector;
- $\boldsymbol{\varepsilon}^p$ = vector of principal strain;
- $\boldsymbol{\sigma}, \boldsymbol{\sigma}'$ = stress tensor and vector;
- σ_1^e = maximum principal stress when concrete is assumed to be elastic material;
- τ = bond stress;
- τ_0, τ_r = bond strength and residual bond strength; and
- ν = Poisson's ratio of virgin concrete.

References

- Bazant, Z. P., and Oh, B. H. (1983). "Crack band theory for fracture of concrete." *Mater. Constr.*, 16(93), 155–177.
- "Examples of the design of concrete structures." *FIP handbook on practical design*, Thomas Telford, London.
- Hayashi, S., and Kokusho, S. (1982). "Fundamental study of bond between deformed bar and concrete." *Proc., AIJ*.
- Herrmann, L. R. (1978). "Finite element analysis of contact problems." *J. Eng. Mech. Div., Am. Soc. Civ. Eng.* 104(5), 1043–1057.
- Keuser, M., and Mehlhorn, G. (1987). "Finite element models for bond problems." *J. Struct. Eng.*, 113(10), 2160–2173.
- Liu, Y. (2003). "Computational experiment of reinforced concrete structural elements using damage mechanics." PhD thesis, Nanyang Technological Univ., Singapore.
- Lourenço, P. B., and Rots, J. G. (1997). "Multisurface interface model for analysis of masonry structures." *J. Eng. Mech.*, 123(7), 660–668.
- Lu, X. Z. (2000). "Experimental study on the damage evolution of rebar-concrete interface." *Final Year Project Rep.*, School of Civil and Environmental Engineering, Nanyang Technological Univ., Singapore.
- Lundgren, K., and Gylltoft, K. (2000). "A model for the bond between concrete and reinforcement." *Mag. Concrete Res.*, 52(1), 53–63.
- Maekawa, K., and Qureshi, J. (1997). "Computational model for reinforcing bar embedded in concrete under combined axial pullout and transverse displacement." *Proc., JCI*, 15(2), 1249–1254.
- Malvar, L. J. (1992). "Bond of reinforcement under controlled confinement." *ACI Mater. J.*, 89(6), 593–601.
- Ngo, D., and Scordelis, A. C. (1967). "Finite element analysis of reinforced concrete beams." *ACI J. Proc.*, 64(3), 152–163.
- Rots, J. G. (1988). "Computational modeling of concrete failure." Thesis, Delft Univ. of Technology, Delft, The Netherlands.
- Schafer, H. (1975). "A contribution to the solution of contact problems with the aid of bond elements." *Comput. Methods Appl. Mech. Eng.*, 6, 335–354.
- Soh, C. K., Chiew, S. P., and Dong, Y. X. (1999). "Damage model for concrete-steel interface." *J. Eng. Mech.*, 125(8), 979–983.
- Stankowski, T., Runesson, K., and Sture, S. (1993a). "Fracture and slip of interfaces in cementitious composites. I: Characteristics." *J. Eng. Mech.*, 119(2), 292–314.
- Stankowski, T., Runesson, K., and Sture, S. (1993b). "Fracture and slip of interfaces in cementitious composites. II: Implementation." *J. Eng. Mech.*, 119(2), 315–327.
- "User information: Version K7." (1997). *MARC: Volume A*, Marc Analysis Research Corporation, Palo Alto, Calif.